Ashdin Publishing
Bioceramics Development and Applications
Vol. 1 (2011), Article ID D110165, 4 pages
doi:10.4303/bda/D110165

Research Article

Initial Adhesion Behavior of Fibroblasts onto Hydroxyapatite Nanocrystals

Motohiro Tagaya,[1,2] Toshiyuki Ikoma,[1] Taro Takemura,[1] Satoshi Migita,[1] Mitsuhiro Okuda,[1] Tomohiko Yoshioka,[2] Nobutaka Hanagata,[1] and Junzo Tanaka[2]

[1]*National Institute for Materials Science, Tsukuba, Ibaraki 305-0047, Japan*
[2]*School of Science & Engineering, Tokyo Institute of Technology, Tokyo 152-8550, Japan*
Address correspondence to Motohiro Tagaya, tagaya.motohiro@nims.go.jp

Received 14 January 2011; Accepted 3 February 2011

Abstract The initial adhesion, spreading and cytoskeleton changes of fibroblast NIH3T3 cells onto hydroxyapatite (HAp) and oxidized poly(styrene) (PSox) sensors pre-adsorbed fetal bovine serum were analyzed by using a quartz crystal microbalance with dissipation technique and an atomic force microscopy (AFM). The frequency shift (Δf) and the dissipation shift (ΔD) curves on HAp nanocrystals showed the decrease in Δf with increasing ΔD for 80 min and the subsequent increase in Δf with decreasing ΔD, while those on PSox showed the decrease in Δf for 120 min with increasing ΔD for 50 min and then with subsequent decreasing ΔD. The different adhesion behavior dependent on the surfaces was attributed to the cell-surface interactions; the cells on HAp had rough fibrous pseudopods and those on PSox had dense particulate pseudopods. The different structures indicated that the cytoskeleton changes and the rearrangement of the extracellular matrix at the interface caused the different adhesion behavior.

Keywords hydroxyapatite; QCM-D; soft interface; cell adhesion; protein adsorption

1 Introduction

Hydroxyapatite ($Ca_{10}(PO_4)_6(OH)_2$; HAp) shows a good biocompatibility for fibroblasts; down growth of percutaneous device [1] and catheter [2] is improved by using HAp sintered body and coatings. The biocompatible features are attributed to the surface property of HAp. Therefore, understanding protein adsorption and cell adhesion onto HAp surface is of great importance for controlling cell functions.

To detect the interfacial phenomena, a quartz crystal microbalance with dissipation (QCM-D) technique is one of excellent *in situ* analytical methods. The HAp sensor applicable for the QCM-D technique was recently fabricated with an electrophoretic deposition method in our group to analyze protein adsorption [3,6]. Although a few studies about the cell adhesion on the surfaces have been reported, no cell adhesion behavior on the HAp surface with the QCM-D technique has been investigated [4,5].

In this study, the QCM-D technique and atomic force microscopy (AFM) were employed for the initial cell adhesion, spreading and cytoskeleton change of fibroblast NIH3T3 cells onto HAp and oxidized poly(styrene) (PSox) sensors.

2 Materials and methods

Gold (QSX-301) and poly(styrene) sensors (QSX-305, film thickness: 40 nm) were purchased from Q-Sense Inc. Fetal bovine serum (FBS, Model number: 12603C, Lot No. 6D0975: SAFC Bioscience Co. Ltd.), Dulbecco's minimum essential medium (DMEM: Invitrogen Co. Ltd.), phosphate buffer saline (PBS: Dulbecco Co. Ltd.) and formaldehyde (37%, Wako Co. Ltd.) were used. Fibroblast NIH3T3 cells (RCB1862) were provided by Riken BioResource Center.

The HAp sensor was fabricated by the electrophoretic deposition method based on our previous reports [3,6]. The poly(styrene) sensor oxidized by a UV/OZONE treatment (PSox) was used as a reference. The fibroblast cells were cultured in a plastic culture flask (BD Bioscience, USA) at 37 °C in a humidified atmosphere of 5% CO_2. The cells washed with 15 mL of PBS and treated with 1 mL of trypsin-EDTA for 5 min were dispersed into in 10% FBS/DMEM. The cell suspensions in the 10 vol% FBS/DMEM were adjusted at the concentrations of 2.5×10^4, 5.0×10^4, 7.5×10^4 and 10.0×10^4 cells/mL.

QCM-D (D300, Q-Sense AB) measurements were performed at 37.0 ± 0.05 °C by real time *in situ* monitoring of Δf and ΔD at 15 MHz. The Δf was transformed to $\Delta f_{n=3}/3$ as the fundamental frequency of 5 MHz. The viscoelastic property of the FBS adlayers was evaluated by

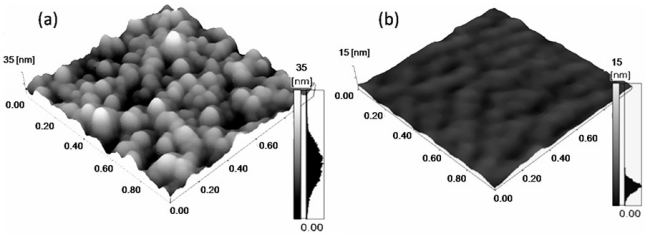

Figure 1: AFM topographic images of (a) HAp and (b) PSox sensors.

a saturated $\Delta D/(\Delta f_{n=3}/3)$ value from the $\Delta D - \Delta f_{n=3}/3$ plot. The adsorption of FBS dispersed into DMEM at 10 vol% was measured for 1 hr after stabilizing a baseline of serum-free DMEM. Subsequently, the cell suspensions were seeded at 0.5 mL on the FBS-adlayer on HAp or PSox sensors, and cultured for 2 hr in air, and rinsed with 0.5 mL of 10 vol% FBS/DMEM. The cultured cells on the sensors were fixed with 3.7 vol% formaldehyde in PBS. The cells fixed were soaked into 1 mL of ethanol/ultrapure water series at 50, 60, 70, 80, 90, 100 vol% for each 5 min, and were into 1 mL of t-butyl alcohol three times at 37 °C. The samples were kept at 4 °C for 0.5 h and then freeze-dried at 4 °C for 4–5 h.

The wettability of the sensors was evaluated in air by a sessile drop method of distilled water with a contact angle meter (CA-W200, Kyowa Interface Science Inc.). The morphology of the cells cultured on the sensors was observed with a confocal laser scanning microscope (CLSM: OLS-3000, OLYMPUS Inc.). The number, area, and volume of the adherent cells were calculated from the 2-D and the 3-D images ($n = 10$) obtained with scanning Z-range at a z-step of 10 nm. The sensor surfaces before and after the cell adhesion were observed with an atomic force microscope (AFM: SPM-9500, Shimazu Inc.). Silicon nitride probe mounted on cantilever (OMCL-AC160TS, OLYMPUS Inc.) was employed for the dynamic mode. The surface roughness was calculated by root mean squares (RMS) in the Z-range images.

3 Results and discussion

Figure 1 shows the AFM topographic images of HAp and PSox sensors. The HAp surface deposited on the gold sensor and the PSox surface have a RMS value of 4.4 ± 0.4 nm and 0.4 ± 0.2 nm. The contact angles of HAp and PSox sensors showed hydrophilicity at $48.7 \pm 2.1°$ and $34.6 \pm 4.1°$.

The FBS adsorption at 60 min caused the $\Delta f_{n=3}/3$ and ΔD shifts at -39.5 ± 3.3 Hz and $+2.2 \pm 0.2 \times 10^{-6}$ on HAp, and at -76.5 ± 9.9 Hz and $+6.3 \pm 2.1 \times 10^{-6}$ on PSox. The saturated $\Delta D/(\Delta f_{n=3}/3)$ was $-3.2 \pm 1.8 \times 10^{-8}$ for HAp and $-3.9 \pm 1.7 \times 10^{-8}$ for PSox (data not shown). While the adsorbed amount of FBS on PSox was larger than that on HAp, the viscoelastic property, judging from the saturated $\Delta D/(\Delta f_{n=3}/3)$, was almost same on HAp and PSox.

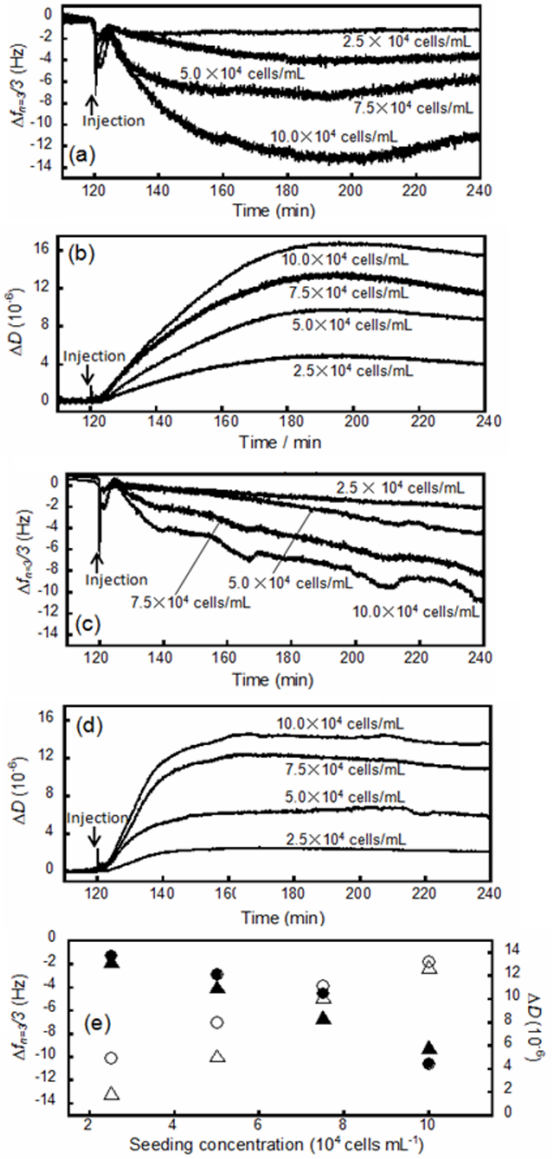

Figure 2: (a), (c) $\Delta f_{n=3}/3$ and (b), (d) ΔD curves of fibroblasts onto (a), (b) HAp and (c), (d) PSox sensors for the first 2 hr (the seeding concentration: 2.5×10^4, 5.0×10^4, 7.5×10^4, 10.0×10^4 cells mL^{-1}). (e): $\Delta f_{n=3}/3$ and (b), (d) ΔD values with the seeding concentration.

Figure 2 shows $\Delta f_{n=3}/3$ and ΔD curves against the acquired times of fibroblasts adhesion onto the adlayer of FBS on HAp and PSox sensors. The $\Delta f_{n=3}/3$ and ΔD curves of the cell adhesion on HAp showed the decrease in the $\Delta f_{n=3}/3$ with increasing the ΔD for 80 min and the increase in the $\Delta f_{n=3}/3$ with decreasing the ΔD (Figures 2(a) and (b)). On the contrary, the cell adhesion on PSox showed the monotonic decrease in the

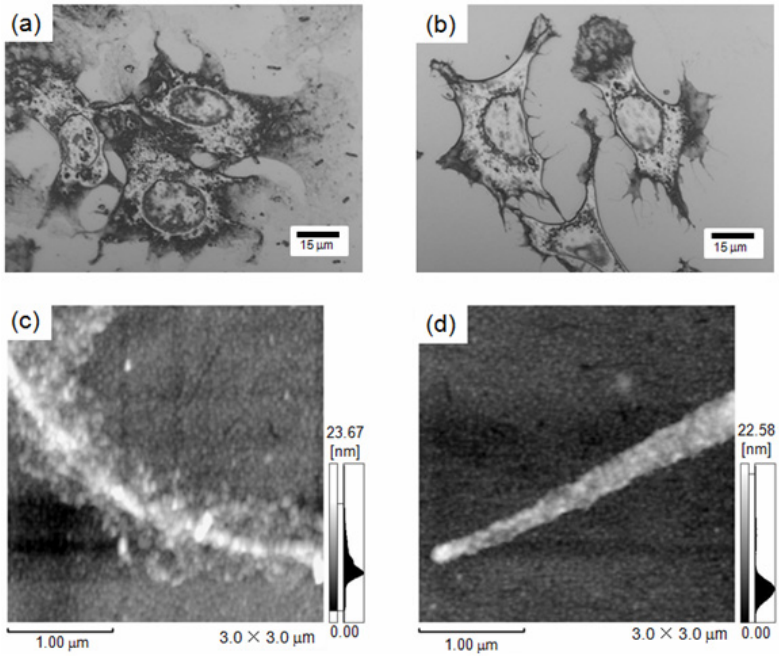

Figure 3: (a), (b) CLSM images of the cultured cells and (c), (d) AFM topographic images of the pseudodia on (a), (c) HAp and (b), (d) PSox.

$\Delta f_{n=3}/3$ for 120 min with increasing the ΔD for 50 min and subsequently decreasing the ΔD (Figures 2(c) and (d)). These results clearly indicate the different adhesion process depending on the surfaces. The decrease in mass and viscoelastic property for fibroblast adhesion onto the PSox and Ta has been reported [4,5]; the cell spreading and cytoskeleton changes depending surface properties would lead to an increase in rigidity of the adherent cells and result in the decrease in the ΔD. Therefore, the different adhesion process depending on the surface was successfully *in situ* monitored by the QCM-D technique, and the cell-surface interactions through the protein adsorption were distinguished.

The $\Delta f_{n=3}/3$ values at 120 min for the concentrations at 2.5×10^4, 5.0×10^4, 7.5×10^4, 10.0×10^4 cells mL^{-1} were -1.2 Hz, -2.9 Hz, -4.5 Hz and -10.5 Hz on HAp and -1.7 Hz, -3.9 Hz, -6.5 Hz and -9.1 Hz on PSox, and the ΔD values were $+4.9 \times 10^{-6}$, $+8.0 \times 10^{-6}$, $+11.1 \times 10^{-6}$ and $+13.2 \times 10^{-6}$ on HAp and $+1.9 \times 10^{-6}$, $+5.2 \times 10^{-6}$, $+10.2 \times 10^{-6}$ and $+12.8 \times 10^{-6}$ on PSox. The $\Delta f_{n=3}/3$ and ΔD values at 120 min show the liner relationship with the seeding concentration (Figure 2(e)). The numbers of adherent cell (N) at 120 min, counted with the light microscopy, was 1.2×10^3, 1.8×10^3, 2.1×10^3 and 2.6×10^3 cells/cm^2 on the HAp, and 1.2×10^3, 1.5×10^3, 1.7×10^3 and 1.9×10^3 cells/cm^2 on the PSox for the corresponding cell concentrations. The Δf showed linear relationship with the N: the $\Delta f/N$ is -6.3×10^{-3} ($R = 0.93$) and -10.8×10^{-3} ($R = 0.93$) Hz $\cdot$ cell^{-1} $\cdot$ cm^{-2}. The previous report on the fibroblasts onto the serum-adsorbed gold surface showed -1.3×10^{-3} Hz $\cdot$ cell^{-1} $\cdot$ cm^{-2} of $\Delta f/N$ at 5 hr [7]. The $\Delta f/N$ values were smaller than a real mass of cells, which could be attributed to (1) the height of cell nucleus in micrometer order, (2) the penetration depths of the resonating waves of the quartz crystal, and (3) the slip of the FBS adlayer attenuating the f-shift from adherent cells.

Figure 3 shows the CLSM images of the cells cultured on HAp and PSox, and the AFM topographic images of pseudodia. The CLSM images showed that the cell morphology on PSox was more anisotropic than that on HAp; the cells on HAp expanded the planular and fibrous pseudodia, while those on PSox expanded the fibrous pseudodia (Figures 3(a) and 3(b)). The cell volume was 45 ± 15 μm^3 on HAp and was 61 ± 20 μm^3 on PSox at 2 h. The AFM images showed that the cells on HAp had rough pseudopod at the height of 15–20 nm and those on PSox had dense particulate pseudopods at the height of 10–15 nm (Figures 3(c) and 3(d)). The different structures of the pseudopod on the cell adhesion points indicated that the cytoskeleton changes and the rearrangement of extracellular matrix at the interfaces caused the different binding behavior.

4 Conclusions

In this study, the QCM-D technique was employed for evaluating the initial adhesion, spreading and cytoskeleton changes of fibroblast on HAp and PSox sensors. The Δf and ΔD curves on HAp and PSox showed the different

behavior on the surfaces, indicating the adhesion process affected by cell-surface interactions through the protein adsorption. The Δf and ΔD showed the linear relationship against the number of adherent cell. The AFM images showed the different pseudopod structures depending on the cell adhesion places. Therefore, these results indicate that the cytoskeleton changes and the rearrangement of extracellular matrix at the interfaces caused the different binding behavior.

References

[1] H. Aoki, M. Akao, Y. Shin, T. Tsuzi, and T. Togawa, *Sintered hydroxyapatite for a percutaneous device and its clinical application*, MED Prog Technol, 12 (1987), 213–220.

[2] T. Furuzono, M. Ueki, H. Kitamura, K. Oka, and E. Imai, *Histological reaction of sintered nanohydroxyapatite-coated cuff and its fibroblast-like cell hybrid for an indwelling catheter*, J Biomed Mater Res B Appl Biomater, 89 (2009), 77–85.

[3] T. Ikoma, M. Tagaya, N. Hanagata, T. Yoshioka, D. Chakarov, B. Kasemo, et al., *Protein adsorption on hydroxyapatite nanosensors with different crystal sizes studied in situ by a quartz crystal microbalance with the dissipation method*, J Am Ceram Soc, 92 (2009), 1125–1128.

[4] M. S. Lord, C. Modin, M. Foss, M. Duch, A. Simmons, F. S. Pedersen, et al., *Monitoring cell adhesion on tantalum and oxidised polystyrene using a quartz crystal microbalance with dissipation*, Biomaterials, 27 (2006), 4529–4537.

[5] ———, *Extracellular matrix remodelling during cell adhesion monitored by the quartz crystal microbalance*, Biomaterials, 29 (2008), 2581–2587.

[6] A. Monkawa, T. Ikoma, S. Yunoki, T. Yoshioka, J. Tanaka, D. Chakarov, et al., *Fabrication of hydroxyapatite ultra-thin layer on gold surface and its application for quartz crystal microbalance technique*, Biomaterials, 27 (2006), 5748–5754.

[7] J. Wegener, A. Janshoff, and H.-J. Galla, *Cell adhesion monitoring using a quartz crystal microbalance: comparative analysis of different mammalian cell lines*, Eur Biophys J, 28 (1998), 26–37.